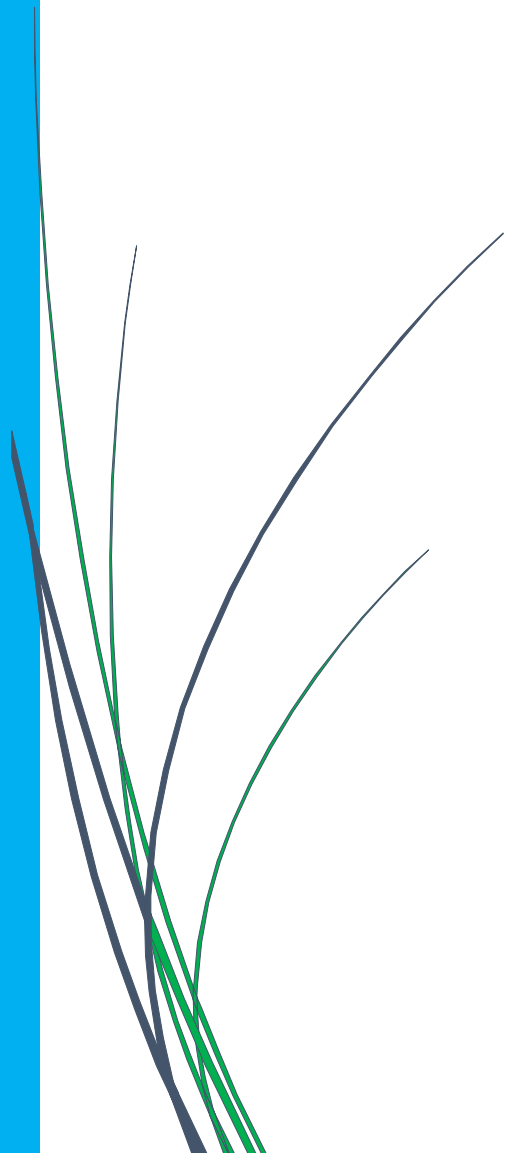


Chapter:7

Effect of pre-reaction treatment on Co/CeO₂ nanocube for ESR



7.1 Introduction

The active metal with CeO₂ support has better oxygen storage and exchange behaviour comparative to other supports [325]. These properties diminish the chance of catalyst to get deactivated by carbon deposition during ESR [252]. Mostly, the noble metals with CeO₂ support were studied, but those catalysts were very costly increasing overall cost of hydrogen generation [18, 26, 35, 36, 118, 149, 212, 228, 229, 236, 275, 310, 326-329]. Among non-noble catalysts, both the Ni and Co have been investigated with CeO₂ and they have shown comparable hydrogen generation. Cobalt based catalyst were with various support initially studied by Llorca et al. [39] and further Co/CeO₂ catalyst has been studied by several authors for ESR reaction because of its low temperature activity to generate hydrogen [37, 39, 68, 181, 185, 253, 330-338]. Soyakal et al. [186, 339] investigated the role of size and morphology for the activity of Co/CeO₂ during ESR. They found that CeO₂ with nano-cube morphology and abundant (110) plane has superior performance for ESR comparable to nano-rod with Co based catalyst. Whereas, the study of Moraes et al. suggested that the morphology of nano CeO₂ didn't affect the product distribution in case of Ni/CeO₂ [122]. The Co/CeO₂-nano cube was reported for high selectivity of hydrogen at 693K in presence of excess water (Molar ratio of ethanol: water =1:21) by Lin et al. [68].

Each ESR study has reported the reduction of active metal oxides in the H₂ atmosphere before the reaction to attain metallic state. But recently, the studies of an active catalyst at different oxidation states were also reported for significant variation in product distribution. It was also reported that during ESR, the oxidation states of Co get changed [340, 341]. The different oxidation states balance of Co (0) and Co (II) was found to be significant by two different research groups [256, 312]. However, in each study, the different oxidation states were studied either attaining the strong interaction

with support by high temperature calcination or in reduction of time duration. In both the cases, the Co (II) state was very minutely changed. Whereas, the study over bare Co_3O_4 suggested that even during ESR, the oxidation states of Co got altered. It indicates that in case of strong metal support interaction, the effect of different oxidation states balance may be different compared to the presence of active metals with less strong support interaction. Moreover, the oxidation state of Ce considerably changes Ce^{3+} and Ce^{4+} in redox atmosphere [288, 295]. The different oxidation states of metals can be attained by variation of pre-treatment condition. If it has positive impact, then interval feeding of particular gas mixture during ESR can resolve the issue of complete transformation of Cobalt in Co^0 state. Therefore redox atmosphere pretreatment may be effective achieve different oxidation states.

The pre-treatment of catalyst in redox atmosphere was not investigated till now. In this study, the experiment was performed to find out the effect of pre-treatment condition in redox atmosphere and complete reduction atmosphere by product gas distribution analysis and physio-chemical properties of the catalysts. Hence, this study may show insight on a path for the behavior of catalyst in redox atmosphere during ESR. The CO and air was used first time to find out its pre-treatment effect on the catalyst for ESR performance. The CO is a harmful gas and by using it for pre-treatment condition with air, it gets oxidized into CO_2 , which is less harmful. On the basis of aforementioned literature survey, it is necessary to analyze the effect of pre-treatment conditions on the Co/ CeO_2 nano-cube over ethanol conversion and selectivity of gases during ESR.

7.2 Experimental

7.2.1 Catalyst preparation

The CeO_2 nanocube was prepared as described by Mai et al. [342]. Briefly, the aqueous solution of $\text{Ce}(\text{NO}_3)_2 \cdot 6\text{H}_2\text{O}$ was precipitated with NaOH with a vigorous stirring

conditions, and it was kept in Teflon lined stainless steel vessels for 24h into the furnace at 453K. After cooling at room temperature the mixture was centrifuged in Remi PR24 centrifuge at 14500 rpm for 5 minutes. The sample was washed with double distilled water and ethanol three times separately, and obtained compound was calcined at 773K for 2h. The calcined sample was impregnated with $\text{Co}(\text{NO}_3)_2 \cdot 6\text{H}_2\text{O}$ solution prepared in ethanol because it was recently reported to be better impregnation medium compared to water by Song and Ozkan [343]. The impregnation solution contains cobalt in a stoichiometric condition such that it contains 10% of Co/CeO_2 . The agitation was performed for 3h at room temperature, and then slowly temperature was increased to obtain the fuzziness in the mixture. It was dried in an oven overnight and then calcined at 823K for 3h. Thereafter, the obtained $\text{Co}_3\text{O}_4/\text{CeO}_2$ was treated in different pre-treatment conditions.

Each pre-treatment was performed in a quartz reactor having diameter 9mm by preparing a bed using quartz wool at the center of the reactor. The mass of catalyst was taken 1g for each pretreatment condition. The pure H_2 treatment of prepared catalyst was done to reduce the Co_3O_4 into Co^0 state ($\text{Co}/\text{CeO}_2\text{-H}$). Pre-treatment with pure H_2 (99.999%) was performed at 723K at a feed rate of 20ml/h for 2h. Two other samples were prepared in redox atmospheric (H_2 with air and CO with air) conditions. The sample treated with H_2 with air and CO with air were denoted as $\text{Co}/\text{CeO}_2\text{-HA}$ and $\text{Co}/\text{CeO}_2\text{-CA}$ respectively. The flow rate ratio (H_2 : Air and CO : Air) was kept constant (1:10) for both pre-treatment conditions and it was performed at temperature 723K for 2h. After the treatment, it was cooled to room temperature in the inert atmosphere and was stored in desiccator for further characterization and experimental observation.

7.2.2 ESR performance test

ESR reaction was performed in vertical quartz reactor having internal diameter 9 mm. 100 mg of catalyst was kept on quartz wool bed prepared at center of the reactor. To find out the temperature during reaction, thermocouple was kept at the outer wall of reactor. The stoichiometric ratio of water and ethanol (3:1) was fed into the preheater kept at constant temperature of 473K. The feed rate of ethanol water mixture was kept 4ml/h. Each experiment was performed within 1h separately at each temperature, because the oxidation states of Ce and Co varied with time during ESR [288].

7.3 Results and discussion

7.3.1 Characterization studies

7.3.1.1 Textural analysis

The surface area of CeO₂-nanocube was found 41.9 m²/g and pore volume was found 0.071 ml/g. The surface area and pore volume of Co/CeO₂-nanocube was found 35.7 m²/g and 0.069 ml/g. It was little lesser than pure CeO₂ nanocube because of impregnation of Co over CeO₂ surface.

7.3.1.2 XRD analysis

Figure 7.1 depicts the rietveld refined data of CeO₂ by FULLPROF having chi square value 3.84. The prepared structure (from VESTA software) shows that cubic structure of CeO₂, predominantly with (111) plane. The peaks are present at 2 θ value of 28.54°, 33.07°, 47.47°, 56.33°, 59.07°, 69.40°, 76.68° and 79.06° were in agreement of JCPDS 81-0792. The complete reduction atmosphere has shown α -Co formation having 2 θ value 44.22° and 75.86° (JCPDS 89-4307) for Co/CeO₂-H catalyst whereas, Co₃O₄ formation occurred for both Co/CeO₂-HA and Co/CeO₂-CA. The 2 θ values 31.27°, 36.85°, 44.81°, 55.65°, 59.35°, 65.23°, 77.34° and 78.40° were matched with JCPDS 42-1467 among which, 31.27°, 55.65°, 77.34° and 78.40° coincided with values of CeO₂.

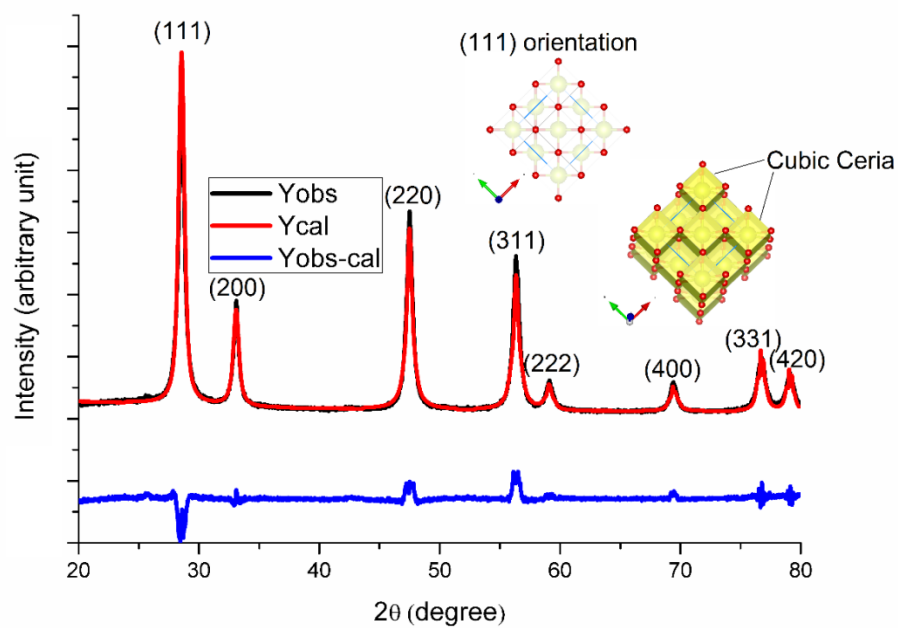


Figure 7.1 Rietveld refinement analysis and prepared crystal structure of nanocube CeO_2 .

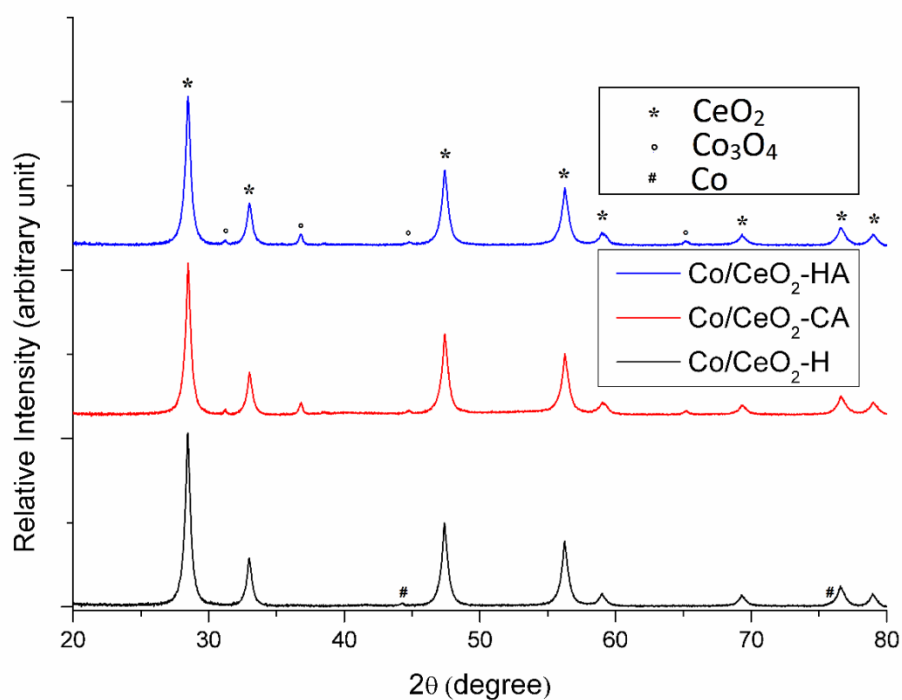


Figure 7.2 HR-XRD of $\text{Co/CeO}_2\text{-H}$, $\text{Co/CeO}_2\text{-CA}$ and $\text{Co/CeO}_2\text{-HA}$ catalysts.

Therefore, separate peaks are absent at those regions as represented in Figure 7.2. The phase of Co was found Cubic in case of each treated catalyst and it contradicts the work of Lin et al.[344].

7.3.1.3 FT-IR analysis

Comparative ATR-FTIR analysis of each catalyst was presented in Figure 7.3. From the Figure, it is clear that peaks at 664 cm^{-1} were found commonly for Co/CeO₂-CA and Co/CeO₂-HA catalysts. It indicates that the Co₃O₄ state of cobalt persists in redox atmosphere. Whereas, in case of Co/CeO₂-H catalyst the peak at 664 cm^{-1} was absent, which is obvious because of complete reduction of Co₃O₄ into Co⁰. These results are also in agreement with HR-XRD results of each catalyst. The wavenumber region $600\text{--}530\text{ cm}^{-1}$ contains four small and sharp peaks for Co/CeO₂-CA compared to Co/CeO₂-HA Co/CeO₂-H.

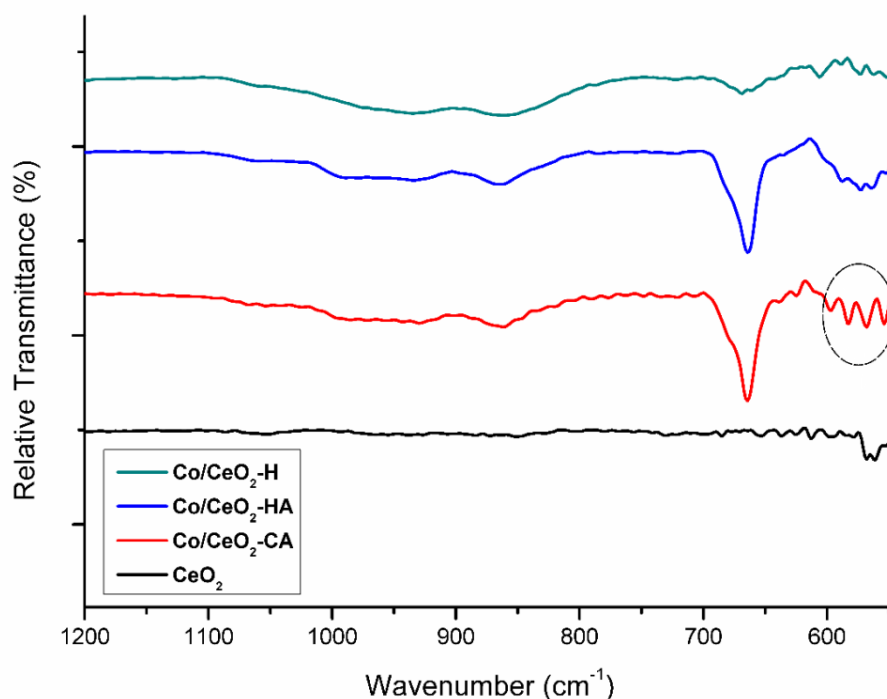


Figure 7.3 FT-IR spectra of Co/CeO₂-CA, Co/CeO₂-HA, Co/CeO₂-H and CeO₂.

It is clear by comparative analysis of FTIR that 565 and 553 cm^{-1} regions belong to CeO_2 , whereas two more peaks near to 600 and 580 cm^{-1} may be considered due to cobalt interaction with Ce. Because these regions are completely absent in CeO_2 but are more or less present in each pre-treatment conditions. The peaks were found more intense in that region for $\text{Co/CeO}_2\text{-CA}$ catalyst. It indicates the metallic interaction of catalyst treated with Co and air get affected more comparative to other treatment conditions. The redox atmosphere treatment with different gases has different consequence regarding interactions among active metal.

7.3.1.4 Morphology analysis

Figure 7.4 represents the TEM, HR-TEM, AFM and SAED pattern of Co/CeO_2 -nanocube in altered pre-treatment atmosphere. The AFM image (Figure 7.4j) of CeO_2 has shown its dimension 40 nm x 100nm x 100 nm (h x l x b) with grooves on the surface. Whereas, the average particle size calculated from the TEM images of Figure 7.4 (a, b and c) were found 20-30nm. It indicates that particles are not completely separated out and so the grooves on the surface were observed in AFM images. An almost cubical surface like morphology retention can also be seen in AFM image. The cubical morphology and the particle size were persistent for each treatment condition. The redox reactions (Co with air and H_2 with Air) and the reduction reaction conditions were exothermic reactions. Hence, it was concluded that even in exothermic reaction condition, size and morphology of particle is not affected. The planer analysis of SAED patterns are in agreement with the XRD data of each catalysts. The planer analysis by SAED patterns, HR-TEM image, and HR-XRD did not not shown any plane deformation changes for CeO_2 . The marked d spacing value (1.56 Å and 1.1 Å) in HR-TEM images can be assigned for CeO_2 which were commonly observed for each pre-treated catalyst. However, the SAED patterns were almost found similar for $\text{Co/CeO}_2\text{-CA}$ (Fig.4d) and

Co/CeO₂-HA (Fig.4e) but, noticeably different for Co/CeO₂-H (Fig. 4f). It is obvious because Co₃O₄ by reduction get converted into metallic Co. Hence, the HR-TEM image, d-spacing value of 1.7 Å and 1.2 Å were found for Co and Co₃O₄ respectively.

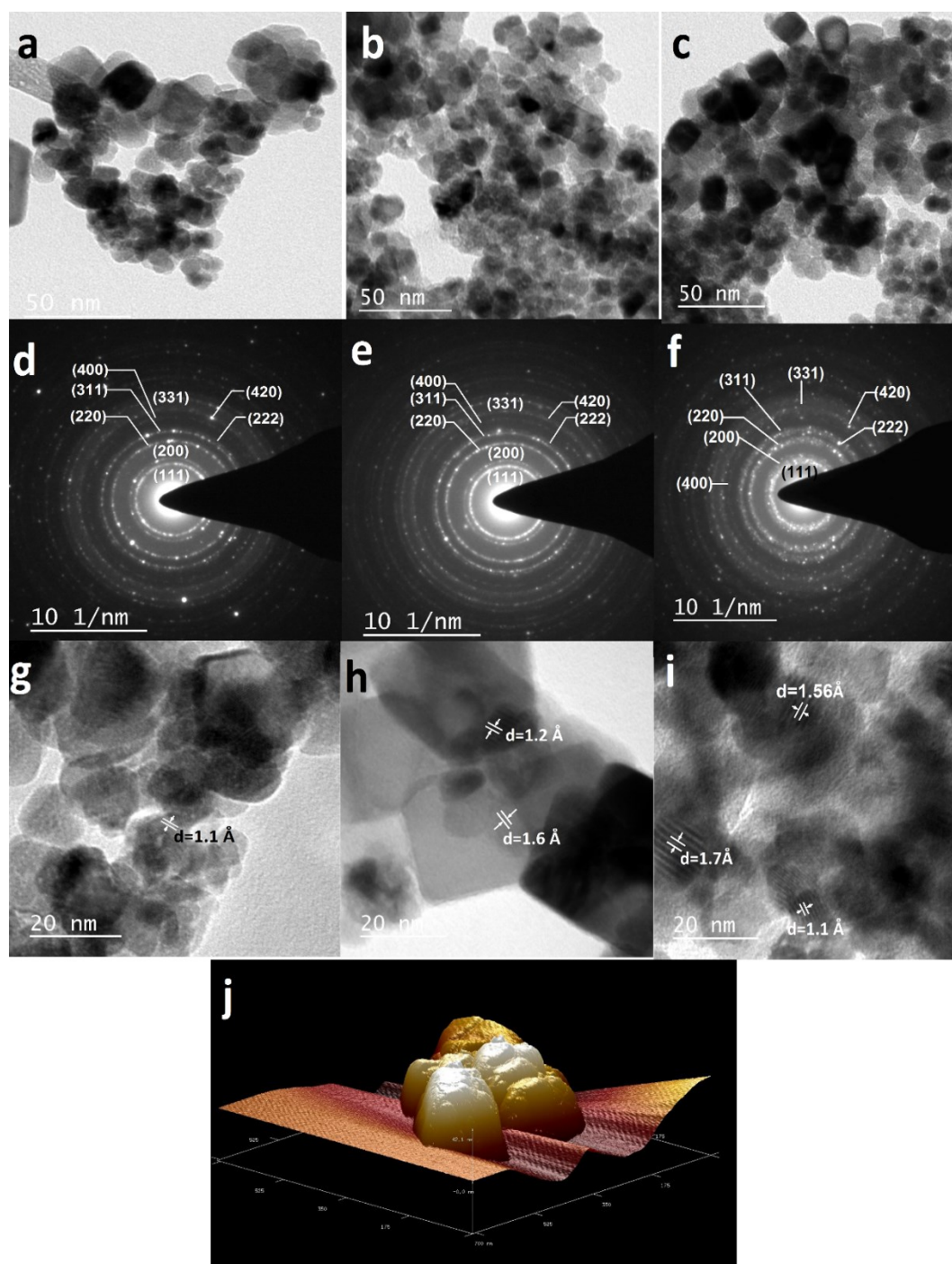


Figure 7.4 TEM image, SAED pattern and HR-TEM images of Co/CeO₂-CA (a, d and g), Co/CeO₂-HA (b, e and h), Co/CeO₂-H (c, f and i) and AFM image (j) of CeO₂.

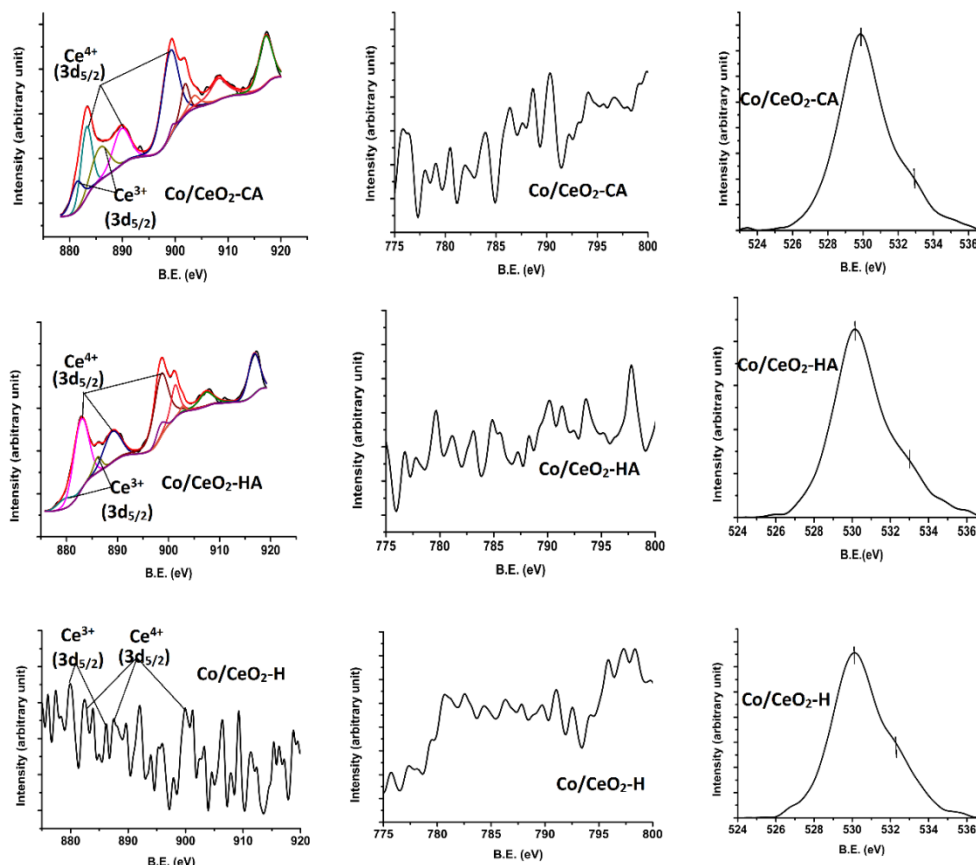


Figure 7.5 XPS analysis of Ce, Co and O for Co/CeO₂-CA, Co/CeO₂-HA and Co/CeO₂-H catalysts.

7.3.1.5 XPS analysis

The nano size CeO₂ is more prominent for reduction as compared to micro sized [288] and it can be analyzed with XPS data. The XPS of Ce contains three doublet in case of Ce⁴⁺ state and two doublet for Ce³⁺ state [151, 253, 326, 345, 346]. The extent of reduction determines the state of CeO₂ as Ce_xO_y (x= 1 and 2, y=2,3,1.5 or 1.8) condition as reported by Flege et al. [347] and so there is probability of number of peaks in case of different oxidation and reduction conditions. The XPS data deconvolution were performed for Ce of Co/CeO₂-CA and Co/CeO₂-HA catalysts. The analysis suggests that the Ce³⁺ state was more abundantly formed in case of Co/CeO₂-CA catalyst. The area of Ce³⁺ state for Co/CeO₂-CA was more than three times at the binding energy 885.7 eV and 904.1 eV compared to Co/CeO₂-HA. This binding energy had been assigned for Ce

(III) $3d^9 4f^1 O 2p^6$ state. The area was also found double at binding energy 880.5 eV and 899.3 eV and both of the peaks assigned for Ce(III) $3d^9 4f^2 O 2p^5$ state[253].

The concentration of Ce^{3+} and Ce^{4+} was found to be 9.94% and 90.06% respectively for Co/CeO₂-HA. In the 9.94%, total area of Ce^{3+} , the area of Ce (III) $3d^9 4f^2 O 2p^5$ and Ce(III) $3d^9 4f^1 O 2p^6$ state were 5.14% and 4.80% respectively. In case of Co/CeO₂-CA, Ce^{3+} and Ce^{4+} concentration were found as 25.05% and 74.95% respectively. In the 25.05% total area of Ce^{3+} , the area of Ce (III) $3d^9 4f^2 O 2p^5$ was 9.85% and area of Ce (III) $3d^9 4f^1 O 2p^6$ state was found 15.20%. Therefore, the Ce^{3+} concentration increment of Ce (III) $3d^9 4f^1 O 2p^6$ state for Co/CeO₂-CA was found three times compared to Co/CeO₂-HA. It was also found interesting that in case of Co/CeO₂-CA, among triplet state of Ce^{4+} , only the area of Ce (IV) $3d^9 4f^2 O 2p^4$ was reduced to half as compared to Co/CeO₂-HA, whereas other states have about common area contribution. All of the Ce oxidation state analysis indicates that CO with air is highly active in reduction of Ce^{4+} by taking the electron from Ce comparative to oxygen.

The complete reduction condition can lead to Ce_xO_y states, which can be observed in the XPS data peaks of Co/CeO₂-H. It contains the similar peaks at common binding energy observed for Co/CeO₂-CA and Co/CeO₂-HA beside those peaks a number of small peaks were observed due to Ce_xO_y states. The XPS analysis of Ce indicates that pretreatment conditions significantly affect the oxidation state of catalyst support CeO₂ and it may have different aspects in ESR performance.

The XPS data of Co for each catalysts are complicated because of different oxidation states and satellite peaks. The Co₃O₄ has spinel phase and it has Co^{3+} as well as Co^{2+} state and so, unable to deconvolute properly with XPS peak. However the graph has been presented in Figure 7.5, where it is clear that the graph was almost common for Co/CeO₂-CA and Co/CeO₂-HA but completely different for Co/CeO₂-H due to abundant

Co⁰ state. The oxygen can be presented in three different form of bridging and non-bridging in each catalyst. The first peak for non-bridging can be assigned to 530.1 eV and peak at 533.3 eV can be assigned for bridging oxygen.

7.3.2 ESR performance test

The ethanol conversion and selectivity of product gases with temperature were represented in Figure 7.6. The ESR performance study showed that Co/CeO₂-H has similar ethanol conversion as Co/CeO₂-CA. Nonetheless, the product gas selectivity was different for both catalysts. The optimum temperature of catalytic activity was found 823K for each catalyst. At this temperature, the ethanol conversion was 94% for Co/CeO₂-CA and Co/CeO₂-H but it was only 30% for Co/CeO₂-HA. In case of Co/CeO₂-CA and Co/CeO₂-HA, the atmospheric reaction condition was redox but the gas species used were different. Hence, it might have happened due to inhibition effect of hydroxyl species formed during redox reaction condition of H₂ and air [295].

The CH₃CHO and C₂H₄ were two double carbon containing products in each pre-treatment condition. The selectivity of CH₃CHO decreases with increasing temperature and completely checked for Co/CeO₂-CA and Co/CeO₂-H at temperature 773K. Whereas, CH₃CHO was found at each temperature for Co/CeO₂-HA. The C₂H₄ was found at each temperature for each catalyst but their selectivity was very less. However, the C₂H₄ selectivity was highest for Co/CeO₂-H and lowest for Co/CeO₂-HA. It is possible due to dehydration reaction, which is facilitated on CeO₂ surfaces. The presence of these two products indicates the dehydrogenation and dehydration reaction pathway adopted by each pre-treatment conditions of Co/CeO₂. The CH₃CHO decomposition leads to CH₄ and CO formation. It is clear from the Figure 7.6 that the selectivity of CO and CO₂ was increasing with temperature but the CH₄ selectivity was not comparable to CO. It indicates that the steam reforming of methane may happen at a higher temperature.

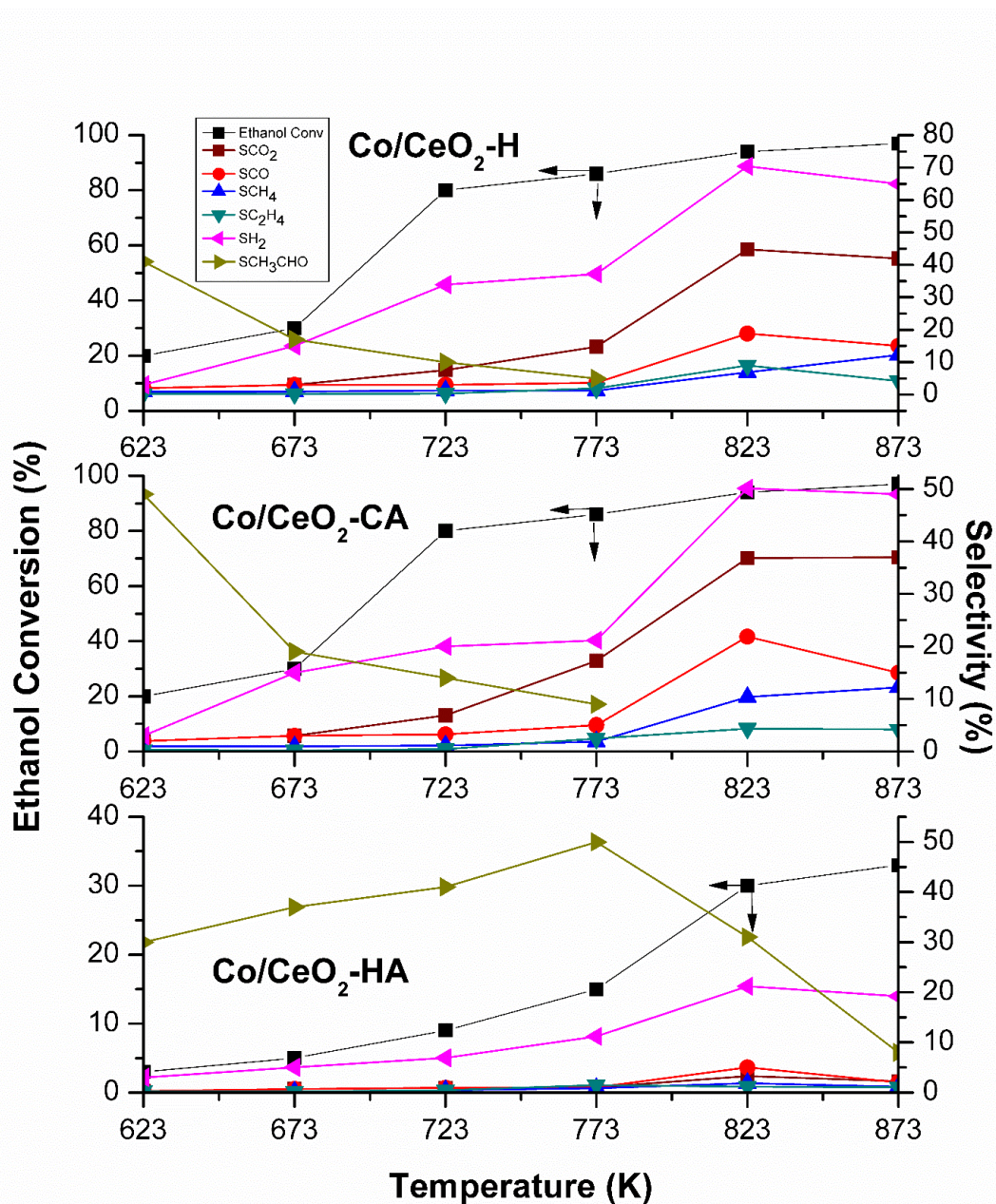


Figure 7.6 ESR performance activity of Co/CeO₂ at different pre-treatment conditions.

The hydrogen gas selectivity was 70% for Co/CeO₂-H and 50% for Co/CeO₂-CA. The CH₄ selectivity was higher for Co/CeO₂-CA, and hydrogen gas selectivity was lesser as compared to Co/CeO₂-H. Therefore, ethanol conversion by Co/CeO₂-H was found to have comparable performance with Co/CeO₂-CA, but the product gas selectivity was different.

The HR-XRD and FTIR studies have shown that the oxidation states Co are almost similar in Co/CeO₂-CA and Co/CeO₂-HA, whereas the oxidation states of Ce vary significantly in each case. It indicates that the different oxidation states of Ce either Ce³⁺ or Ce²⁺ affect the catalytic properties of Co/CeO₂ based catalyst significantly. The XPS studies confirm that the affinity of Ce towards redox reaction with H₂ and CO along with air is different and hence, their catalytic behavior was also different.

7.4 Conclusion

However, the ethanol conversion is almost completed at 823K for both Co/CeO₂-H and Co/CeO₂-CA. The selectivity of hydrogen was found 50% and 70% for Co/CeO₂-CA and Co/CeO₂-H respectively. It occurred due to variation in oxidation states of active metals. The redox atmosphere pre-treatment by CO with air was found better as compared to H₂ with air but H₂ reduction treatment is found most effective for ESR.